December 1978

Perturbation theory in a strong-interaction regime with application to 4d-subshell spectra of Ba and La

Göran Wendin
Chalmers University of Technology, Göteborg, Sweden, goran.wendin@mc2.chalmers.se

Anthony F. Starace
University of Nebraska-Lincoln, astarace1@unl.edu

Published in *Journal of Physics B: Atomic and Molecular Physics* **11**:24 (December 28, 1978), pp. 4119–4134.
http://www.iop.org/EJ/journal/JPhysB

Submitted March 14, 1978; revised July 24, 1978.

Perturbation theory in a strong-interaction regime with application to 4d-subshell spectra of Ba and La

Göran Wendin

Institute of Theoretical Physics, Chalmers University of Technology, Fack, S-402 20 Göteborg 5, Sweden

Anthony F. Starace

Behlen Laboratory of Physics, University of Nebraska–Lincoln, Lincoln, Nebraska 68588 USA
(Alfred P. Sloan Foundation Fellow)

Abstract

We investigate the behavior of a bound electron–hole excitation in an energy region where the response of the system is highly resonant and shows strong collective behavior. Formulae for calculating discrete energy levels and wavefunctions are presented for the case where the perturbation is strong enough to change the nodal structure of the perturbed wavefunctions relative to that of the unperturbed wavefunctions. This change in nodal structure requires a renaming of the associated atomic states. Neglect of such renaming is shown to have been at the root of a recent controversy between differing interpretations, based on alternative calculational procedures, of the 4d-subshell photoionization spectra of Ba and La. It is demonstrated explicitly that these alternative calculational procedures are equivalent and that their interpretations are consistent.

1. Introduction

In an optical absorption process bound or quasibound electron–hole pairs can be excited and, from a physical point of view, such electron–hole pairs are elementary excitations, *i.e.* eigenstates or near-eigenstates of the total system. In a calculation, however, one usually starts from a simple one-electron zero-order basis set describing the electron–hole pair as dynamically decoupled from the rest of the system. In the presence of a residual electron-electron interaction the zero-order electron–hole excitation polarizes the system and induces relaxation effects and is thus turned into an effective physical excitation. These effects can be represented formally as perturbations of the members of the zero-order basis set.

In this paper we present an appropriate formulation for calculating discrete energy levels and wavefunctions in the case of strong perturbations between members of a zero-order basis set. In such a case Wendin (1976b) has shown that the nodal structure of the zero-order basis set may be altered, thus requiring a change in the naming of the improved wavefunctions and energy levels. Neglect of this required renaming has led to a recent controversy over the merits of alternative calculational procedures which should, in principle, be equivalent (Dehmer *et al.* 1971, Hansen

et al. 1975). A main purpose of the present paper is to demonstrate this equivalence numerically, using the formulae presented here, for those elements that have been involved in the controversy: barium and lanthanum. In addition, we illustrate the strength of the perturbation in these two elements by comparing the effective local potentials seen by an excited electron before and after the perturbation is switched on. In the remainder of this introduction we review the controversy mentioned above in order to motivate the calculations for barium and lanthanum presented below.

The controversy relates to the theoretical interpretation by Dehmer *et al.* (Dehmer *et al.* 1971, Starace 1972, 1974, Sugar 1972, Dehmer and Starace 1972) of the 4d-subshell photoabsorption spectra of the rare earths ($57 \leq Z \leq 70$). In brief, Dehmer *et al.* (1971) interpreted these experimental spectra (Zimkina *et al.* 1967, Fomichev *et al.* 1967, Haensel *et al.* 1970, Gudat and Kunz 1972) as resulting from a simple two-step process: photoexcitation of a 4d-subshell electron into the 4f subshell, *i.e.*

$$4d^{10}4f^{N} \xrightarrow[\text{photoexcitation}]{} 4d^{9}4f^{N+1} \tag{1.1}$$

where N is the occupation number of the 4f subshell, followed by autoionization of the various terms of the $4d^{9}4f^{N+1}$ configuration into the alternative continuum channels $4d^{9}4f^{N} + e^{-}$, *i.e.*

$$4d^{9}4f^{N+1} \xrightarrow[\text{autoionization}]{} 4d^{9}4f^{N} + e^{-} \ (l = 3 \text{ or } 1) \tag{1.2}$$

where the continuum electron has predominantly an orbital angular momentum $l = 3$. This theory assumed the use of a *single* basis set of one-electron orbitals (such as that provided by an average-of-configuration Hartree-Fock calculation). The energies of the various term levels of the intermediate configuration $4d^{9}4f^{N+1}$ were obtained by diagonalizing the energy matrix within this configuration (Sugar 1972, Starace 1974). Electrostatic interactions within the intermediate configuration were found to be so strong that many of the higher-term levels were shifted above the $4d^{9}4f^{N}$ threshold, as defined of course in the one-electron basis. Finally, the decay of each of the term levels of the $4d^{9}4f^{N+1}$ configuration lying above threshold, *via* reaction (1.2), was treated by ordinary techniques of scattering theory (Starace 1972, Dehmer and Starace 1972). This theoretical interpretation of Dehmer *et al.* (1971) was bolstered by the excellent agreement between the observed spectroscopic structure and the predictions of Sugar (1972) for the term energies and oscillator strengths of the intermediate configuration $4d^{9}4f^{N+1}$.

A controversy arose when the above theory was used by experimentalists to interpret their data on the 4d-subshell photoabsorption spectrum of barium (Connerade and Mansfield 1974, Ederer *et al.* 1975, Rabe *et al.* 1974). Wendin (1973b) had earlier carried out an RPAE calculation for the dominant transition from the barium 4d subshell,

$$\text{Ba } 4d^{10} \xrightarrow[\text{photoabsorption}]{} \text{Ba } 4d^{9}\epsilon f(^{1}P), \tag{1.3}$$

starting from an average-of-configuration Hartree-Fock basis. He found that the 4d $\rightarrow$ 4f transition in the ^{1}P channel is so strongly coupled to the 4d $\rightarrow \epsilon$f transitions, that one should speak of a "giant dipole resonance" in the continuum. This calculation of Wendin (1973b) showed that the 4d-subshell photoabsorption spectrum was similar to that of the rare earths and thus could also be interpreted—and in fact was—along the lines of Dehmer *et al.* (1971): that is, in an average-of-configuration Hartree-Fock basis almost all the absorption strength from the 4d subshell is concentrated in the transition

$$\text{Ba } 4d^{10} \xrightarrow[\text{photoabsorption}]{} \text{Ba } 4d^9 4f. \tag{1.4}$$

Electrostatic and spin-orbit interactions split the ^1P, ^3P, and ^3D term levels of the $4d^9 4f$ configurations and shift the optically allowed ^1P term level above the $4d^9$ threshold. The high-lying $4d^9 4f\ ^1P$ level then decays primarily to the continuum channel 4d94f ^1P by autoionization, producing the broad resonance in the continuum that is observed experimentally. This interpretation of the experiment was criticized by Hansen *et al.* (1975), who calculated the cross section for reaction (1.3) starting from a restricted Hartree-Fock basis set (*i.e.*, a basis set in which the electrostatic interactions appropriate for the channel under consideration are included in the differential equation used to generate the one-electron f orbitals). They also found a large peak in the continuum. However, in contradiction to the interpretation of Dehmer *et al.* (1971), they found that the $4d^9 4f\ ^1P$ level lies below the $4d^9$ threshold and that the corresponding transition has almost no oscillator strength (Fliflet *et al.* 1975)!

Wendin (1976b) indicated the resolution to these contradictory interpretations. He suggested the following revision of the theoretical interpretation of Dehmer *et al.* (1971): reactions (1.1) and (1.2) describe properly the shift of *oscillator strength* from the 4d → 4f transition to the continuum once the electrostatic interactions are taken into account; however, in addition, these same strong electrostatic interactions cause the 4f orbital to mix with the other discrete *n*f orbitals in such a way that the perturbed *n*f orbitals each lose one node. Thus, for example, the unperturbed 5f orbital becomes a 4f orbital after it is perturbed by the electrostatic interactions. Hence there is a level re-ordering which results in a 4f level below threshold having very little oscillator strength, since its wavefunction is similar to the zero-order 5f orbital except that it has no node. Moreover, this 4f orbital below threshold was suggested by Wendin (1976b) to be identical to the one calculated directly by Hansen *et al.* (1975).

In this paper we show that these suggestions of Wendin (1976b) are indeed correct, to the limits of our numerical accuracy, for both barium and lanthanum 4d-subshell photoabsorption. That is, we give a detailed demonstration of how perturbation theory can be used to go from the average-of-configuration single-particle states to the $4d^9 nf\ ^1P$ states in a strong-interaction regime (in which the perturbation alters the nodal structure of the initial basis wavefunctions). Hence we conclude that one may start either from an average-of-configuration Hartree-Fock basis set (Dehmer *et al.* 1971, Wendin 1973a, 1974) or from a restricted Hartree-Fock basis set (Hansen *et al.* 1975, Wendin 1976a) when calculating photoabsorption spectra, wavefunctions, and energy levels for barium, the rare earths, or other systems having strong perturbations in the average-of-configuration Hartree-Fock basis. Furthermore, the theoretical interpretations of these photoabsorption processes, while somewhat dependent on the initial basis set chosen, are nevertheless consistent with each other.

2. Wavefunctions and energy levels in a strong-interaction regime

In this section we review some basic expressions describing the coupling of a particular level to the remaining excitation spectrum. Consider a Hamiltonian H, which is partitioned according to $H = H_0 + V$, where H_0 defines a basis set of excited states according to

$$H_0|n\rangle_0 = \omega_n^0 |n\rangle. \tag{2.1}$$

As indicated in equation (2.1), the energy ω_n^0 is measured with respect to the energy of the subshell being excited so that ω_n^0 coincides with the photon energy. When the residual interaction V is introduced, the zero-order basis states may be said to become "dressed up" to effective excitations, and, if the residual interaction is strong, these new "effective" states may have very different properties from the unperturbed ones. More explicitly, the energy eigenstates $|\omega_n\rangle$ of the full Hamiltonian H, where

$$H|\omega_n\rangle = \omega_n |\omega_n\rangle \tag{2.2}$$

may be written in terms of the reaction matrix of Brillouin-Wigner perturbation theory as (see, *e.g.*, Kumar 1962, Starace 1972, 1974, Wendin 1976a,b)*

$$V_{n'n}(\omega) = V_{n'n} - \sum\!\!\!\!\!\!\int_m \frac{V_{n'm}V_{mn}(\omega)}{\omega_m^0 - \omega} \tag{2.3}$$

Here the reaction matrix is obtained as the solution of the equation

$$V_{n'n}(\omega) = V_{n'n} - \sum\!\!\!\!\!\!\int_m \frac{V_{n'm}V_{mn}(\omega)}{\omega_m^0 - \omega} \tag{2.4}$$

and the energy ω_n is obtained as the solution of the equation

$$\omega_n = \omega_n^0 + V_{nn}(\omega_n) \tag{2.5}$$

The normalization factor is obtained from equation (2.3) to be

$$N^2 = 1 + \sum\!\!\!\!\!\!\int_{n'} \frac{|V_{n'n}(\omega_n)|^2}{(\omega_{n'}^0 - \omega_n)^2}. \tag{2.6}$$

However, as shown in Appendix 1, the normalization may also be calculated from the simpler expression

$$N^2 = 1 - (\partial V_{nn}(\omega)/\partial\omega)|_{\omega=\omega_n}. \tag{2.7}$$

In either case, we choose the sign of N so that the resulting wavefunction in equation (2.3) has a positive slope at the origin. In Appendix 2, the connection between the above formulae and those for the atomic polarizability is discussed.

In the case of strong interactions between some of the zero-order basis states and only weak interactions among the rest, the equations above may be rearranged to emphasize the dominant interactions. This rearrangement is carried out, using projection operators, in Appendix 3; alternatively, the rearrangement may be done by a diagrammatic analysis (Wendin 1970, 1974, 1976a). Here we present the results for those physical systems of interest in this paper, barium and lanthanum. In each case, the zero-order basis set $|n\rangle_0$ comprises the Slater determinants for the excited configurations $4d^9nf$, where n extends over both discrete and continuum energies. The one-electron orbitals are calculated in the average-of-configuration Hartree-Fock approximation. The perturbation V consists of those electrostatic interactions between the states $|n\rangle_0$ that arise when each configuration is coupled to a ^1P symmetry. The dominant interactions are those between each state and the $4d^94f$ state, $|4\rangle_0$.

The eigenstate $|\omega_n\rangle$ in equation (2.3) may be rewritten in a way that emphasizes the dominant interaction between the zero-order states $|n\rangle_0$ and $|4\rangle_0$ as follows (*cf.*

* $\sum\!\!\!\!\!\!\int$ denotes a sum over discrete states and a Cauchy principal-part integration over continuum states. When ω_n is discrete, then $n' \neq n$.

Appendix 3, Wendin 1974, 1976a):

$$|\omega_n\rangle = N^{-1}\left(|\bar{n}\rangle - \frac{|\bar{4}\rangle \bar{V}_{4n}(\omega_n)}{\omega_4^0 + \bar{V}_{44}(\omega_n) - \omega_n}\right). \tag{2.8}$$

In equation (2.8) the interactions between $|n\rangle_0$ or $|4\rangle_0$ and all other states are incorporated in the reduced eigenfunctions and reduced reaction matrix indicated by the bar notation:

$$|\bar{n}\rangle \equiv |n\rangle_0 - \sum_{(m\neq 4)} \frac{|m\rangle_0 \bar{V}_{mn}(\omega_n)}{\omega_m^0 - \omega_n} \tag{2.9}$$

and

$$\bar{V}_{n'n}(\omega) \equiv V_{n'n} - \sum_{(m\neq 4,n)} \frac{V_{n'm}\bar{V}_{mn}(\omega)}{\omega_m^0 - \omega}. \tag{2.10}$$

The energy of the eigenstate $|\omega_n\rangle$ is given by equation (2.5), where the full reaction matrix $V(\omega)$ in that equation is given in terms of the reduced reaction matrix $\bar{V}(\omega)$ according to

$$V_{n'n}(\omega) = \bar{V}_{n'n}(\omega) - \frac{\bar{V}_{n'4}(\omega)\bar{V}_{4n}(\omega)}{\omega_4^0 + \bar{V}_{44}(\omega) - \omega}. \tag{2.11}$$

Our numerical results for the perturbed eigenstates in equation (2.8) are presented in Section 4, but these results may be described qualitatively here. First, the matrix element $\bar{V}_{44}(\omega_n)$ is large, so that the denominator in equation (2.8) is positive. Hence, since $\bar{V}_{44}(\omega_n)$ is also positive,** the coefficient of $|\bar{4}\rangle$ in equation (2.8) is negative, *i.e.*

$$\bar{C}_{4n} \equiv \frac{-\bar{V}_{4n}(\omega_n)}{\omega_4^0 + \bar{V}_{44}(\omega_n) - \omega_n} < 0. \tag{2.12}$$

Furthermore $\bar{C}_{4n}$ is large enough that the sum

$$|\bar{n}\rangle + \bar{C}_{4n}|\bar{4}\rangle \tag{2.13}$$

has a sign opposite to that of $|\bar{n}\rangle$ in the region of the first maximum of $|\bar{n}\rangle$; *i.e.*, $|\omega_n\rangle$ has one fewer node than the state $|\bar{n}\rangle$. In Section 4 we show that $|\omega_n\rangle$, calculated according to equation (2.8), is identical to the restricted Hartree-Fock state with one fewer node in its f orbital, *i.e.*

$$|\omega_n\rangle = |4d^9(n-1)f\ ^1P\rangle_{RHF}. \tag{2.14}$$

The calculations of Wendin (1976b) employed equation (2.8) in the approximation that the reduced reaction matrix elements $\bar{V}_{4n}(\omega_n)$ and $\bar{V}_{44}(\omega_n)$ could be replaced by the bare interaction matrix elements V_{4n} and V_{44}. We find that, indeed, the matrix $\bar{V}(\omega)$ is close to the bare matrix V, but it is necessary to calculate $\bar{V}(\omega)$ in order to demonstrate exactly the equality in equation (2.14).

3. Wavefunctions and their effective local potentials

In this paper we are considering Hartree-Fock (HF) type wavefunctions, obtained from equations of the form

$$\left(-\frac{d^2}{dr^2} + \frac{l(l+1)}{r^2} + V_{nl}^{H}(r) - E\right)P_{nl}(r) = X_{nl}(r). \tag{3.1}$$

** Coupling of the $4d^9nf$ excitations to a ^1P state introduces a large repulsive electrostatic interaction. As a result. both the diagonal and the off-diagonal matrix elements of the residual interaction $V_{nn'} \simeq \langle 4dnf|1/r_{12}|n'f4d\rangle$ will be positive, and so also will the effective interaction $\bar{V}_{4n}(\omega)$.

Here, r is expressed in atomic units, energies and potentials in rydbergs, and the wavefunctions obey the normalization condition

$$\int_0^\infty P_{nl}^2(r)\mathrm{d}r = 1.$$

A straightforward way to obtain a *local potential* giving the wavefunction in equation (3.1) is through the relation (*cf.* Slater 1951, Cooper 1962, Hansen 1972)

$$V_{nl}(r) = V_{nl}^{\mathrm{H}}(r) - \frac{X_{nl}(r)}{P_{nl}(r)}. \tag{3.2}$$

At the nodes of $P_{nl}(r)$, the potential $V_{nl}(r)$ is singular, but otherwise it is a smooth, well behaved function of r. In an HF program the quantities $V_{nl}^{\mathrm{H}}(r)$ and $X_{nl}(r)$ are available directly, and one can then obtain the local potential easily. However, in many cases one has knowledge only of a wavefunction in numerical form. In this case, one can obtain the local potential from (Cadioli *et al.* 1972, Hilton *et al.* 1977)

$$V_{nl}(r) = E - \frac{l(l+1)}{r^2} + \frac{P_{nl}''(r)}{P_{nl}(r)} \qquad \text{(Ryd)}, \tag{3.3}$$

giving the effective local potential

$$V_{nl}^{\mathrm{eff}}(r) = V_{nl}(r) + [l(l+1)/r^2] \qquad \text{(Ryd)}. \tag{3.4}$$

We have used equations (3.3) and (3.4) to obtain potential curves for various states in Ba and La both before and after the strong electrostatic perturbation is switched on. We find that comparison of these effective local potentials permits one to obtain a highly consistent picture of the photoabsorption process in these elements.

4. Application to Ba and La

We have used the equivalent equations (2.3) and (2.8) to calculate the perturbed eigenstates $|\omega_n\rangle$ corresponding to the zero-order state

$$|n\rangle_0 \equiv |4\mathrm{d}^9 n\mathrm{f}\rangle_0 \tag{4.1}$$

in barium and lanthanum.* We have chosen two values for n: $n = 5$ and $n = 6$. It will be convenient to express equation (2.3) in the form

$$|\omega_n\rangle = N^{-1}\left(|n\rangle_0 + \sum_{n'} C_{n'n}(\omega_n)|n'\rangle_0\right) \tag{4.2a}$$

where the coefficient of the zero-order state $|n'\rangle_0$ is

$$C_{n'n}(\omega_n) \equiv -\frac{V_{n'n}(\omega_n)}{\omega_{n'}^0 - \omega_n}. \tag{4.2b}$$

Similarly, equation (2.8) may be expressed as

$$|\omega_n\rangle = N^{-1}(|\bar{n}\rangle + \bar{C}_{4n}(\omega_n)|\bar{4}\rangle) \tag{4.3}$$

* Note that in lanthanum we treat interactions between the 5d electron and the other electrons in an average way, *i.e.,* we spherically average the La ground state so that it may be considered to be in a ^{1}S term level. This averaging, done for convenience, is not expected to affect greatly the excitations from the 4d subshell.

where the reduced wavefunctions $|\bar{n}\rangle$ and $|\bar{4}\rangle$ of the two-dimensional model space are defined by equation (2.9), and where the coefficient $\bar{C}_{4n}(\omega_n)$ is defined by equation (2.12). Note that the equality in equation (A3.13a) implies that

$$\bar{C}_{4n}(\omega) = C_{4n}(\omega) \tag{4.4a}$$

for any ω, or explicitly,

$$\frac{\bar{V}_{4n}(\omega)}{\omega_4^0 - \omega + \bar{V}_{44}(\omega)} = \frac{V_{4n}(\omega)}{\omega_n^0 - \omega}. \tag{4.4b}$$

The first step in calculating the perturbed wavefunctions $|\omega_n\rangle$ for $n = 5$ and $n = 6$ is to solve equation (2.5) by iteration for the perturbed energy levels ω_n. The results are given in Table 1, where in column (2) the orbital energy E_n is obtained from

$$E_n = \omega_{n+1} + E_{4d} \tag{4.5}$$

where $E_{4d}^{Ba} = -8{,}003$ Ryd and $E_{4d}^{La} = -9.107$ Ryd. Equation (4.5) is the expression for the energy corresponding to equation (2.14) for the wavefunctions; that is, since the perturbed state $|\omega_{n+1}\rangle$ has one fewer node than the average-of-configuration zero-order state $|n+1\rangle_0$, we associate the perturbed energy ω_{n+1} with the configuration $4d^9nf(^1P)$ instead of $4d^9(n+1)f(^1P)$. As seen in Table 1, these synthesized orbital energies compare almost identically with the orbital energies calculated directly.

Using the computed values for ω_n, equations (4.2) or (4.3) were used to compute the $(n-1)$f orbital wavefunction. In Figure 1(a) we compare the 4f ^{1}P (synthesized) orbital wavefunction with the unperturbed 4f HF_{av} and 5f HF_{av} orbitals in Ba. The corresponding orbitals in La are shown in Figure 2(a). The figures show clearly that for radii $r \gtrsim 9$ au the 4f ^{1}P (synthesized) orbital is close to the 5f HF_{av} orbital. In the region 1 au $\leq r \leq 4$ au, however, the 5f HF_{av} orbital has a node. This node is removed by the ^{1}P electrostatic interaction which mixes the 4f HF_{av} and 5f HF_{av} orbitals. The mixing coefficient $C_{45}(\omega_5)$is –0.062 in Ba and –0.169 in La. Differences between the 4f ^{1}P (synthesized) orbitals and the 4f ^{1}P (direct) orbitals cannot be discerned on the scale of Figure l(a) and are barely discernible in Figure 2(a). Similar results (not shown) were obtained for the 5f ^{1}P orbital.

The strength of the electrostatic interaction in the ^{1}P channel is shown dramatically by a comparison of the effective potentials seen by the nf HF_{av} orbitals and the nf ^{1}P (synthesized) orbitals. These potentials, calculated according to equations (3.3) and (3.4), are quite insensitive to the value of n. The effective potentials for Ba are shown in Figure 1(b) and those for La in Figure 2(b).* One sees in each case that the HF_{av} effective potentials are wider and deeper. Each has a potential barrier in the neighborhood of $r = 2$ au, although the barrier in Ba is much larger than the one in La. The ^{1}P (synthesized) effective potentials, on the other hand, are much narrower and slightly less deep. The effect of this drastic change in potential is that the 4f level is pushed up in energy and out in radius: whereas the $4f_{av}$ orbital energy is –0.74 Ryd: the 4f ^{1}P orbital energy is –0.06 Ryd; whereas the $4f_{av}$ orbital peaks at $r \simeq 0.6$ au, the 4f ^{1}P orbital peaks at $r \simeq 15$ au. Rather curiously, the effective ^{1}P potential in Ba has a *double* potential barrier, one maximum lying at $r \simeq 0.9$ and the other at

* The singularity in the $5f_{av}$ potential is no artifact but is a consequence of the node in the wavefunction and the nonlocality of the HF potential (see equation (3.2)). There are no singularities in the $4f_{av}$ and the 4f ^{1}P potentials because the corresponding wavefunctions have zero nodes. The singularity in the 5f ^{1}P potential occurs at $r > 25$ au and is very weak. In order to use the local potentials for approximate calculations at arbitrary energies these singularities have to be removed.

Table 1. Orbital energies of the nf electron in the configuration $4d^9nf(^1P)$ as calculated in the Hartree-Fock approximation, either directly, or else indirectly by proper synthesis of average-of-configuration wavefunctions.

E_n (Ryd)	Ba			La		
	(1)[a]	(2)[b]	(3)[c]	(1)[a]	(2)[b]	(3)[c]
n	HF_{av}	HF ^1P(synth)	HF ^1P(direct)	HF_{av}	HF ^1P(synth)	HF ^1P(direct)
4f	−0.74660	−0.06574	−0.06574	−1.32569	−0.06692	−0.06699
5f	−0.064660	−0.04256	−0.04255	−0.06425	−0.04473	−0.04436
6f	−0.04160			−0.04133		

a Column (1) gives nf energies as calculated in an average-of-configuration Hartree-Fock computation for the configuration $4d^9nf$.
b Column (2) gives the nf orbital energy E_n calculated according to equation (4.5).
c Column (3) gives the nf orbital energy obtained directly from an HF(^1P) computation for the configuration $4d^9nf(^1P)$.

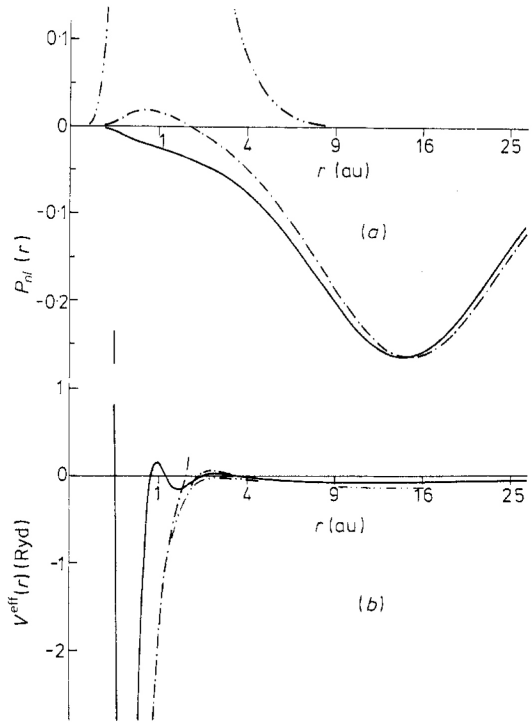

Figure 1. Wavefunctions and effective local potentials for atomic Ba. (**a**) Wavefunctions : — ··— ··— ·, 4f HF_{av}; — ·— ·— ·, 5f HF_{av}; — — —, 4f HF ^1P synthesized, which cannot be distinguished from the result of a direct HF calculation on the scale of the figure. (Note that in this figure the phase of the 4f ^1P wavefunction has been reversed for convenient comparison with 5f HF_{av}.) The peak value of the curve — ··— ··— ·· is 0.915 at r = 0.79 au. (**b**)Effective local potentials: — ·— ·— ·, 5f $HF_{av;}$ — ··— ··— ··, 4f HF_{av} (same as 5f HF_{av} for $r \lesssim 1$); ——, 4f, 5f, HF ^1P. For r $\lesssim$ 0.5, all potentials coincide. Curve —— has a minimum of –8.70 Ryd at r = 0.36 au; curve — ·— ·— · has a minimum of –9.75 Ryd at r = 0.40 au.

$r \simeq 2.0$ au. These locations correspond roughly to the positions of maximum amplitude of the 4d and 5p HF_{av} orbitals. Hence the shell structure of Ba is mirrored in the effective potential seen by nf ^1P orbitals. However, no excited orbitals are known to be localized in the intermediate well at $r \simeq 1.4$ au. The greater nuclear attraction in La causes the ^1P effective potential in that element to have a *shoulder* at $r \simeq 1.0$ au instead of a barrier; there is, however, a small barrier at $r \simeq 3.0$ au. As in Ba, these features occur at radii corresponding to the maximum amplitude of the 4d and 5p HF_{av} orbitals.

In Figure 3 we illustrate the relative importance of the various components of the 4f ^1P (synthesized) orbital wavefunction in Ba. Thus both $|5f\rangle_0$ and $\sum_{n'} C_{n'5}(\omega_5)|n'f\rangle_0$ of equation (4.2a) are shown (as well as the dominant term in the summation, $C_{45}(\omega_5)|4f\rangle_0$); their sum

$$N|\omega_5\rangle \equiv N|4d^9 4f\ ^1P\rangle$$

is also shown. The normalization factor is very close to unity: N_{Ba} = 1.0043. Similarly, both $|\bar{5}f\rangle$ and $\bar{C}_{45}(\omega_5)|\bar{4}f\rangle$ of equation (4.3) are shown. They also sum to $N|\omega_5\rangle$.

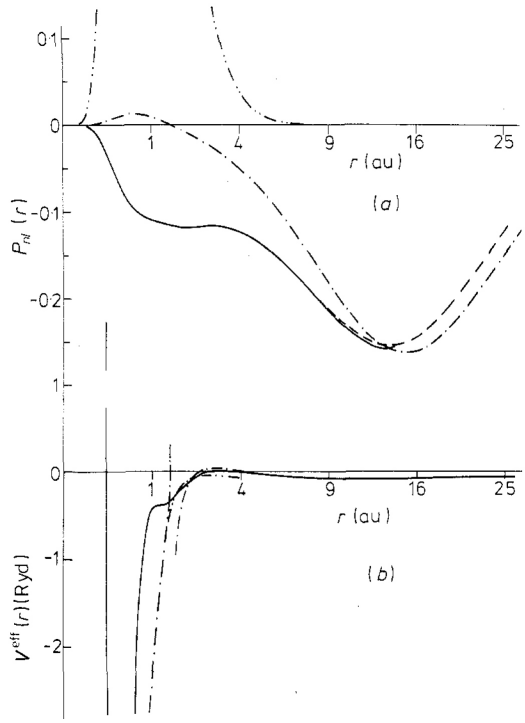

Figure 2. Wavefunctions and effective local potentials for atomic La. (**a**) Wavefunctions : — ··— ··—, 4f HF_{av}; — ·— ·—, 5f $HF_{av;}$ ———, 4f HF ^1P synthesized; — — — —, 4f HF ^1P, direct calculation. (Note that in this figure the phase of the 4f ^1P wavefunction has been reversed for convenient comparison with 5f HF_{av}.) The synthesized and direct curves are closely equal for $r \lesssim 9$. At larger radii, however. the synthesized solution starts to oscillate around the correct one (this might be due to the cut-off of high-frequency components in the basis set). The peak value of the curve — ··— ··— is 0.996 at r = 0.72 au. (**b**) Effective local potentials: — ·— ·—, 5f HF_{av}; — ··— ··—, 4f HF_{av} (same as 5f HF_{av} for $r \lesssim 1$); ———, 4f, 5f HF ^1P. For $r \lesssim 0.5$ all potentials coincide. Curve ——— has a minimum of –10.55 Ryd at r = 0.35 au: curve — ·— ·— has a minimum of –11.45 Ryd at r = 0.38 au.

The arrows indicate the radial positions of the two potential barriers in the ^1P effective potential for Ba. At these locations both $\bar{C}_{45}(\omega_5)|\bar{4f}\rangle$ and $\mathcal{P}_{n'}C_{n'5}(\omega_5)|n'f\rangle_0$ have kinks that result in points of inflection in the 4f ^1P orbital wavefunction. Thus Figure 3 gives firm support to the conjectures of Wendin (1976b), namely that the 4f HF_{av} orbital dominates the behavior of the 4f ^1P orbital at small radii, whereas the 5f HF_{av} orbital dominates the behavior of the 4f ^1P orbital at large radii.

The above discussion may also be extended to the continuum. In synthesizing the ϵf ^1P wavefunctions from average-of-configuration wavefunctions, using equation (4.3) for example, one finds that the inner-well region is dominated by the $|\bar{4f}\rangle$ wavefunction. Since this inner region determines the 4d $\rightarrow$ ϵf transition matrix elements, one has in effect a transfer of the inner-well resonance transition (*i.e.* 4d $\rightarrow$ 4f in the average-of-configuration basis set) to the continuum. It is in this sense that the authors and others say that the 4d photoionization cross section of Ba and La (metals as well as vapor and compounds) is dominated by a 4f resonance.

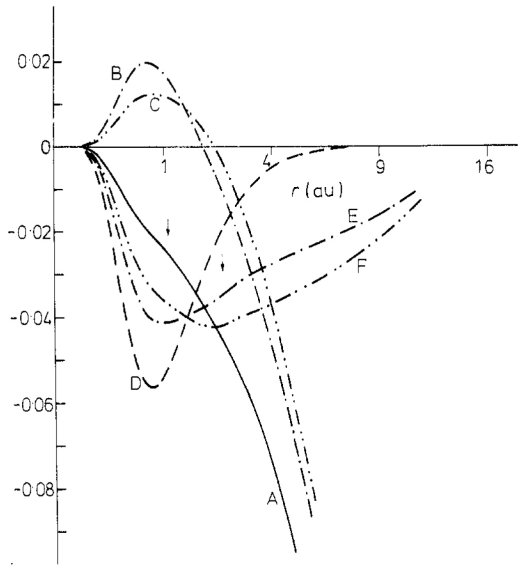

Figure 3. The 4f HF ^{1}P synthesized wavefunction in Ba and its components according to the decompositions in equations (2.3) and (2.8). **A**. $|4f\ \mathrm{HF}\ {}^1\mathrm{P}\rangle$ synthesized (the direct result is well represented by the same curve); **B**. $|5f\rangle_0$: **C**. $|\bar{5}f\rangle$ (equation (2.9)); **D**. $C_{45}(\omega_5)|\underline{4f}\rangle_0$ (equation (4.2)): **E**. $\underline{\not\Sigma}_n C_{n5}(\omega_5)|n\rangle_0 = N|4f\ {}^1\mathrm{P}\rangle - |5f\rangle_0$ (equation (4.2)); **F**. $\underline{C}_{45}(\omega_5)|4f\rangle = N|4f\ {}^1\mathrm{P}\rangle - |\bar{5}f\ \rangle$ (equation (4.3)).

5. Discussion and conclusions

In this paper we have demonstrated the equivalence of two choices of initial basis set for determining wavefunctions and energy levels for certain optically excited configurations in Ba and La. While the direct approach of Hansen *et al.* (1975) is simpler,* the alternative approaches of Dehmer *et al.* (1971) and of Wendin (1973a, 1974) using the reaction matrix give the same results: as was demonstrated by Wendin (1976a). The picture of Wendin (1976b) in which each bound $|n\mathrm{f}\ {}^1\mathrm{P}\rangle$ orbital is considered to result from the perturbation of the $(n+1)$f $\mathrm{HF_{av}}$ orbital by the 4f $\mathrm{HF_{av}}$ orbital is found to be essentially correct; this picture is exact in the sense of equation (4.3) in which the $\mathrm{HF_{av}}$ orbitals are replaced by the reduced orbitals defined by equations (2.9) and (2.10).

We find the behavior of Ba and La atoms to be remarkably similar. This similarity is best demonstrated by the effective potentials shown in Figures 1(b) and 2(b). In each case, the narrowing of the HF ^{1}P effective potential well with respect to the $\mathrm{HF_{av}}$ effective potential well results in the raising of the nf ^{1}P levels relative to the nf $\mathrm{HF_{av}}$ levels and also gives rise to a prominent shape resonance in the continuum that can be thought of as originating from the average-of-configuration 4f level.

In addition, our calculations confirm the recent work of Miller and Dow (1977) in showing that the effective local potentials are approximately independent of the energy of the excited electron in the vicinity of the ionization threshold, *i.e.,* over an energy range of a few rydbergs.

* In a wider perspective this is not true. In order to obtain realistic results, one usually has to account for electron correlations, at least at the level of the random phase approximation and sometimes also including relaxation effects. At such levels of approximation the computational effort is practically independent of the starting point.

Acknowledgments

This work has been supported in part by the Swedish Natural Science Research Council (G.W., A.F.S.) and in part by the U.S. Department of Energy (A.F.S.) under contract number EY-76-S-02-2892. A.F.S. wishes especially to acknowledge the hospitality of the Institute of Theoretical Physics of Chalmers University of Technology, where much of this work was carried out.

Appendix 1. Derivation of equation (2.7)

Differentiation of equation (2.4) gives

$$\frac{\partial V_{nn}(\omega)}{\partial \omega} = -\sum_m \frac{V_{nm}V_{mn}(\omega)}{(\omega_m^0 - \omega)^2} - \sum_m \frac{V_{nm}(\partial V_{mn}(\omega)/\partial\omega)}{(\omega_m^0 - \omega)}. \tag{A1.1}$$

Now, in operator notation, equation (A1.1) may be written

$$\frac{\partial V(\omega)}{\partial \omega} = -V\frac{1}{(H_0 - \omega)^2}V(\omega) - V\frac{1}{(H_0 - \omega)}\frac{\partial V(\omega)}{\partial \omega}. \tag{A1.2}$$

Solving equation (A1.2) for $\partial V(\omega)/\partial\omega$ gives

$$\frac{\partial V(\omega)}{\partial \omega} = -\left(1 + V\frac{1}{(H_0 - \omega)}\right)^{-1} V\frac{1}{(H_0 - \omega)^2}V(\omega). \tag{A1.3}$$

But by inspection of the operator equivalent of equation (2.4), *i.e.*

$$V(\omega) = V - V\frac{1}{(H_0 - \omega)}V(\omega), \tag{A1.4}$$

we find that

$$V(\omega) = \left(1 + V\frac{1}{(H_0 - \omega)}\right)^{-1} V. \tag{A1.5}$$

Substituting equation (A1.5) in equation (A1.4) gives

$$\frac{\partial V(\omega)}{\partial \omega} = -V(\omega)\frac{1}{(H_0 - \omega)^2}V(\omega). \tag{A1.6}$$

The matrix expression for equation (A1.6) is simply the second term on the right-hand side of equation (2.6), which thus proves equation (2.7).

Appendix 2. Relation of equations (2.3) and (2.7) to formulae for the atomic polarizability

One way of obtaining equation (2.3) for the wavefunction is to study the polarizability of the system in the neighborhood of the resonance corresponding to the

appropriate final state:

$$\alpha(\omega) \sim \frac{P_n^2(\omega)}{\omega_n^0 + V_{nn}(\omega) - \omega} + C(\omega). \tag{A2.1}$$

Here $C(\omega)$ is a slowly varying function of ω, the reaction matrix $V_{nn'}(\omega)$ is given by equation (2.4) and the effective dipole matrix element is given by

$$P_n(\omega) = p_n - \$_m \frac{p_m V_{mn}(\omega)}{\omega_m^0 - \omega} \tag{A2.2}$$

and p_n is the reduced dipole matrix element $\langle 4\mathrm{d}||r||n\mathrm{f}\rangle$. The transition probability is given by the residue of the pole in equation (A2.1), *i.e.*

$$|D(\omega_n)|^2 \sim P_n^2(\omega_n)[1 - (\partial V_{nn}(\omega)/\partial\omega)]^{-1}_{\omega=\omega_n} \tag{A2.3}$$

where ω_n is the position of the pole (see equation (2.5)). The corresponding wavefunction can now be obtained by removing the initial state and the dipole operator everywhere from the amplitudes in equation (A2.3), leading to equation (2.3).

As it stands, equation (A2.2) violates charge conservation, and the corresponding wavefunction would not be normalized. However, the normalization factor can easily be obtained from the energy derivative of the effective energy shift $V_{nn}(\omega)$ because the strength of the energy dependence (*i.e.*, the dispersion) is a measure of the mixture of other states into the unperturbed one. Very close to a strong perturbing resonance, like the $|\overline{4}\mathrm{f}\rangle$ in the present case, the unperturbed state may have very low weight, and the normalization factor might become very large, actually showing a resonance (see equations (2.6) and (2.7)). However, in the present case of 4f and 5f levels in Ba and La, the renormalization effect is rather minor.

Appendix 3. Partitioned equations for the reaction matrix and the perturbed wavefunctions

We represent the reaction matrix equation (2.4) in operator form as

$$V(\omega) = \mathrm{V} - V\,GV(\omega) \tag{A3.1}$$

where

$$G \equiv (H_0 - \omega)^{-1}. \tag{A3.2}$$

We define projection operators P and Q in the usual way, *i.e.*

$$P + Q = 1 \tag{A3.3a}$$

$$PQ = QP = 0 \tag{A3.3b}$$

$$P^2 = P \tag{A3.3c}$$

$$Q^2 = Q. \tag{A3.3d}$$

Since P and Q will be defined in terms of eigenstates of H_0, we have that

$$PGQ = QGP = 0. \tag{A3.4}$$

Hence operating with P on both left and right of equation (A3.1), we obtain

$$PV(\omega)P = PVP - PVPGPV(\omega)P - PVQGQV(\omega)P. \tag{A3.5}$$

Similarly, operating with Q on the left and P on the right of equation (A3.1), we obtain

$$QV(\omega)P = QVP - QVPGPV(\omega)P - QVQGQV(\omega)P. \tag{A3.6}$$

From equation (A3.6) we may solve for $GQV(\omega)P$ to obtain

$$GQV(\omega)P = (G^{-1} + QVQ)^{-1}(QVP - QVPGPV(\omega)P). \tag{A3.7}$$

Substituting equation (A3.7) in equation (A3.5) we obtain

$$PV(\omega)P = PVP - PVPGPV(\omega)P - PVQ(G^{-1} + QVQ)^{-1}(QVP - QVPGPV(\omega)P). \tag{A3.8}$$

Equation (A3.8) may be simplified by first using equation (A3.2) to write

$$(G^{-1} + QVQ)^{-1} QVP = (H_0 + QVQ - \omega)^{-1} QVP \tag{A3.9}$$

and secondly defining a new matrix by

$$P\bar{V}(\omega)P \equiv PVP - PVQ(H_0 + QVQ - \omega)^{-1} QVP. \tag{A3.10}$$

Then, substituting equations (A3.9) and (A3.10) in equation (A3.8) gives

$$PV(\omega)P = P\bar{V}(\omega)P - P\bar{V}(\omega)PGPV(\omega)P. \tag{A3.11}$$

Our main results thus far, equations (A3.10) and (A3.11), may be generalized. Equation (A3.11) serves to represent the full reaction matrix $PV(\omega)P$ within the model space P in terms of the reduced reaction matrix, $P\bar{V}(\omega)P$, defined by equation (A3.10). In general, by removing P from left and right of both equations (A3.10) and (A3.11) we have

$$V(\omega) = \bar{V}(\omega) - \bar{V}(\omega)P(H_0 - \omega)^{-1} PV(\omega) \tag{A 3.12a}$$

$$V(\omega) = V - VQ(H_0 + QVQ - \omega)^{-1} QV. \tag{A 3.12b}$$

Now equations (A3.12a,b) may be used to demonstrate the important equalities*

$$(H_0 - \omega)^{-1} PV(\omega) = (H_0 + P\bar{V}(\omega)P - \omega)^{-1} P\bar{V}(\omega) \tag{A 3.13a}$$

$$(H_0 + QVQ - \omega)^{-1} QV = (H_0 - \omega)^{-1} Q\bar{V}(\omega). \tag{A3.13b}$$

Substituting equation (A3.13a) in equation (A3.12a) and equation (A3.13b) in equation (A3.12b), we obtain alternative expressions for $V(\omega)$ and $\bar{V}(\omega)$:

$$V(\omega) = \bar{V}(\omega) - \bar{V}(\omega)P(H_0 + P\bar{V}(\omega)P - \omega)^{-1} P\bar{V}(\omega) \tag{A3.14a}$$

$$\bar{V}(\omega) = V - VQ(H_0 - \omega)^{-1} Q\bar{V}(\omega). \tag{A3.14b}$$

In the remainder of this appendix we use equations (A3.12)–(A3.14) to verify equations (2.8)–(2.11).

Consider the definition

$$P \equiv |4\rangle_{00}\langle 4| + |n\rangle_{00}\langle n| \tag{A3.15}$$

* For example. equation (A3.13a) is obtained by
(1) multiplying equation (A3.12a) from the left by P;
(2) bringing the second term on the right in equation (A3.12a) to the left-hand side to get $[1 + P\bar{V}(\omega)P(H_0 - \omega)^{-1}]PV(\omega) = P\bar{V}(\omega)$;
(3) factoring $(H_0 - \omega)^{-1}$ out of the bracket; and
(4) operating on both sides from the left with $(H_0 - \omega + P\bar{V}(\omega)P)^{-1}$.

i.e., P defines the subspace containing only the two states $|n\rangle_0$ and $|4\rangle_0$. With this definition, equation (2.10) follows directly from equation (A3.14b). Similarly, equation (2.11) follows directly from equation (A3.14a), provided we recall that the state $|n\rangle_0$ is not to be included in the sum over intermediate states, since it is the state whose improved wavefunction we seek.

To prove equations (2.8) and (2.9), we must start from the general equation (2.3), which we write here in the operator form:

$$|\omega_n\rangle = N^{-1}[P - P(H_0 - \omega_n)^{-1} PV(\omega)P - Q(H_0 - \omega_n)^{-1} QV(\omega)P]\,|n\rangle_0. \tag{A 3.16}$$

Substituting equation (A3.7) in equation (A3.16) we obtain

$$|\omega_n\rangle = N^{-1}[P - P(H_0 - \omega_n)^{-1} PV(\omega)P - Q(\mathrm{H}_0 + \mathrm{QVQ} - \omega)^{-1} \times Q(QVP - QVP(H_0 - \omega)^{-1} PV(\omega)P)]\,|n\rangle_0. \tag{A3.17}$$

Substituting equations (A3.13a,b) in equation (A3.17) and defining the operator

$$X \equiv P - Q(H_0 - \omega)^{-1} Q\bar{V}(\omega)P \tag{A3.18}$$

we obtain finally

$$|\omega_n\rangle = N^{-1}[X - XP(H_0 + P\bar{V}(\omega)P - \omega)^{-1} P\bar{V}(\omega)P]\,|n\rangle_0. \tag{A3.19}$$

Comparing equations (A3.18) and (2.9) we see that the states defined with a bar in equation (2.9) are given simply by

$$|\bar{n}\rangle = X\,|n\rangle_0. \tag{A 3.20}$$

Finally, substituting the definition (A3.15) for *P* in equation (A3.19) and remembering that the state $|n\rangle_0$ must be excluded from the summation over intermediate states, we see that (A3.19) reduces to (2.8).

References

Cadioli, B., Pincelli, U., Tosatti, E., Fano, U., and Dehmer, J. L. 1972 *Chem. Phys. Lett.* **17** 15-8

Connerade, J. P., and Mansfield, M. W. D. 1974 *Proc. R. Soc. A* **341** 267-75

Cooper, J. W. 1962 *Phys. Rev.* **128** 681-93

Dehmer, J. L., and Starace, A. F. 1972 *Phys. Rev. B* **5** 1792-6

Dehmer, J. L., Starace, A. F., Fano, U., Sugar, J., and Cooper, J. W. 1971 *Phys. Rev. Lett.* **26** 1521-5

Ederer, D. L., Lucatorto, T. B., Saloman, E. B., Madden, R. P., and Sugar, J. 1975 *J. Phys. B: Atom. Molec. Phys.* **8** L21-5

Fliflet, A., Kelly, H. P., and Hansen, J. E. 1975 *J. Phys. B: Atom. Molec. Phys.* **8** L268-70

Fomichev, V. A., Zimkina, T. M., Gribovskii, S. A., and Zhukova, I. I. 1967 *Fiz. Tverd. Tela* **9** 1490-2 (Transl. 1967 *Sov. Phys.-Solid St.* **9** 1163-5)

Gudat, W., and Kunz, C. 1972 *Phys. Rev. Lett.* **29** 169-72

Haensel, R., Rabe, P., and Sonntag, B. 1970 *Solid St. Commun.* **8** 1845-8

Hansen, J. E. 1972 *J. Phys. B: Atom. Molec. Phys.* **5** 1083-95

Hansen, J. E., Fliflet, A. W., and Kelly, H. P. 1975 *J. Phys. B: Atom. Molec. Phys.* **8** L127-9

Hilton, P. R., Nordholm, S., and Hush, N. S. 1977 *J. Chem. Phys.* **67** 5213-23

Kumar, K. 1962 *Perturbation Theory and the Nuclear Many-Body Problem* (Amsterdam: North-Holland)

Miller, D. L., and Dow, J. D. 1977 *Phys. Lett.* **60A** 16-8

Rabe, P., Radler, K,. and Wolff, H. W. 1974 *Vacuum UV Radiation Physics,* ed. E. E. Koch *et al.* (Berlin: Vieweg-Pergamon) pp. 247-9

Slater, J. C. 1951 *Phys. Rev.* **81** 385-90

Starace, A. F. 1972 *Phys. Rev. B* **5** 1773-84

———. 1974 *J. Phys. B: Atom. Molec. Phys.* **7** 1425

Sugar, J. 1972 *Phys. Rev. B* **5** 1785-92

Wendin, G. 1970 *J. Phys. B: Atom. Molec. Phys.* **3** 455-77

———. 1972 *J. Phys. B: Atom. Molec. Phys.* **5** 110–32

———. 1973a *J. Phys. B: Atom. Molec. Phys.* **6** 42-61

———. 1973b *Phys. Lett.* **46A** 119-20

———. 1974 *Vacuum UV Radiation Physics,* ed. E. E. Koch *et al.* (Berlin: Vieweg-Pergamon) pp. 225-40

———. 1976a *Photoionization and Other Probes of Many-Electron Interactions,* ed. F. J. Wuilleumier, (New York: Plenum) pp. 61-82

———. 1976b *J. Phys. B: Atom. Molec. Phys.* **9** L297-302

Zimkina, T. M., Fomichev, V. A., Gribovskii, S. A., and Zhukova, I. I. 1967 *Fiz. Tverd. Tela* **9** 1447-50 (transl. 1967 *Sov. Phys.-Solid St.* **9** 1128-30)